An Experimental Test of the Discreteness-of-Charge Effect in Positive and Negative Lipid Bilayers†

Anthony P. Winiski,‡ Alan C. McLaughlin,§ Robert V. McDaniel,∥ Moises Eisenberg,⊥ and Stuart McLaughlin*,#

Department of Biochemistry, State University of New York, Stony Brook, New York 11794, Department of Biochemistry and Biophysics, University of Pennsylvania, Philadelphia, Pennsylvania 19104, Biology Department, Brookhaven National Laboratory, Upton, New York 11973, and Departments of Pharmacological Sciences and of Physiology and Biophysics, Health Sciences Center, State University of New York, Stony Brook, New York 11794

Received July 10, 1986; Revised Manuscript Received August 28, 1986

ABSTRACT: The electrostatic properties of charged bilayers and the bilayer component of biological membranes are often described theoretically by assuming the charge is smeared uniformly over the surface. This is one of the fundamental assumptions in the Gouy–Chapman–Stern (GCS) theory. However, the average distance between the charged phospholipids in a typical biological membrane is 2–3 nm, which is 2–3 times the Debye length in a 0.1 M salt solution. Existing discreteness-of-charge theories predict significant deviations from the GCS theory for the adsorption of ions to such membranes. We considered the predictions of the simplest discreteness-of-charge theory [Nelson, A. P., & McQuarrie, D. A. (1975) *J. Theor. Biol. 55*, 13–27], in which the charges are assumed to be fixed in a square lattice and the potential is described by the linearized Poisson–Boltzmann relation. This theory predicts deviations that are larger for counterions than for co-ions and much larger for divalent than for monovalent counterions. We tested these predictions by measuring the adsorption of a fluorescent monovalent anion and a paramagnetic divalent cation to both positive and negative membranes, which we demonstrated experimentally had the same average surface potential. All our experimental results with probes, including those obtained on membranes in the gel rather than in the liquid-crystalline state, agreed with the predictions of the GCS theory rather than with the discreteness-of-charge theory. A simple calculation indicates that the agreement between the experimental results and the predictions of the GCS theory could be due to the finite size of the lipids.

A significant (10–20%) fraction of the phospholipids in many biological membranes bear a net negative charge (White, 1973). These surface charges are located in the polar head groups of lipids, such as phosphatidylserine (PS),[1] and produce an electrostatic potential in the aqueous phase adjacent to the membrane. The electrostatic potential is conventionally described by the Gouy–Chapman theory, which assumes the charge is smeared uniformly over the surface [e.g., McLaughlin (1977)]. This assumption is not true for membranes, and the discrete character of the charges on the phospholipid head groups must influence the properties of the diffuse double layer. Grahame (1958), Barlow and MacDonald (1967), and Levine et al. (1967) reviewed the early discreteness-of-charge theories, which dealt mainly with the inability of the Gouy–Chapman formalism to describe the adsorption of anions to metallic surfaces. Several investigators have more recently adapted these discreteness-of-charge theories to membranes (Cole, 1969; Brown, 1974; Nelson & McQuarrie, 1975; Sauve & Ohki, 1979; Duniec & Thorne, 1983; Belaya & Feigelman, 1985). We consider the simplest of these treatments (Nelson & McQuarrie, 1975) to illustrate the magnitude of the phenomenon.

Nelson and McQuarrie (1975) used the linearized Poisson–Boltzmann equation of Debye–Huckel theory to calculate the electrostatic potential due to a two-dimensional array of surface charges fixed in a square lattice. The potential in the aqueous phase $\psi(r)$ generated by one surface charge q is

$$\psi(r) = [q/(2\pi\epsilon_r\epsilon_0 r)] \exp(-\kappa r) \quad (1)$$

where ϵ_0 is the permittivity of free space, ϵ_r is the dielectric constant of the aqueous phase, $1/\kappa$ is the Debye length, and r is the distance from the charge. This potential is a factor of 2 larger than the conventional Debye–Huckel potential adjacent to an ion in the bulk aqueous phase because we assume the charge is at an interface with a low dielectric medium and the counterions are confined to the aqueous phase. The potential generated by a number of surface charges is calculated by adding the contributions from the individual charges [see eq 32 of Nelson and McQuarrie (1975)]. A result of this calculation is seen in Figure 1 for a membrane with charges in a square lattice. The magnitude of the potential in the aqueous phase a given distance from the surface (e.g., 0.2 nm) is largest near a surface charge (e.g., 152 mV) and smallest in the center of the square lattice (e.g., 8 mV). If we assume the charges are smeared uniformly over the surface, the one-dimensional linearized Poisson–Boltzmann equation (linearized Gouy–Chapman theory) predicts the potential 0.2 nm from the surface is 20 mV.[2] Note that the potential

† This work was supported by National Science Foundation Grant BNS 85-01456, National Institutes of Health Grant GM 24971, and Council for Tobacco Research Grant 1493.

‡ Department of Biochemistry, SUNY.
§ University of Pennsylvania.
∥ Brookhaven National Laboratory.
⊥ Department of Pharmacological Sciences, SUNY.
Department of Physiology and Biophysics, SUNY.

[1] Abbreviations: DDDA, didodecyldimethylammonium bromide; FCCP, carbonyl cyanide *p*-(trifluoromethoxy)phenylhydrazone; DMPC, dimyristoylphosphatidylcholine; DMPG, dimyristoylphosphatidylglycerol; MOPS, 4-morpholinepropanesulfonate; HNS, 2-(*N*-hexadecylamino)-naphthalene-6-sulfonate; HTAC, hexadecyltrimethylammonium chloride; PC, phosphatidylcholine; PG, phosphatidylglycerol; PS, phosphatidylserine; tempamine, 2,2,6,6-tetramethylpiperidine-1-oxyl; TNS, 2-(*p*-toluidinyl)naphthalene-6-sulfonate; EDTA, ethylenediaminetetraacetic acid.

0006-2960/86/0425-8206$01.50/0

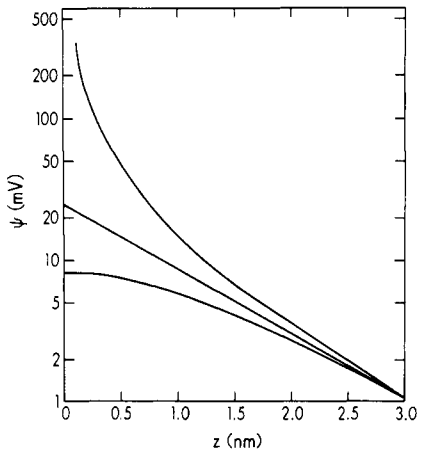

FIGURE 1: Electrostatic potential ψ in aqueous solution adjacent to a positively charged membrane. ψ is plotted as a function of distance z from the membrane, which is located in the xy plane. The straight line is the prediction of linearized Gouy–Chapman theory. The two curves are the predictions of a discreteness-of-charge theory (Nelson & McQuarrie, 1975) when the charges are in a square lattice separated by 3 nm. The upper curve is the potential directly over a surface charge, while the lower curve is the potential in the center of the square lattice. The aqueous solution contains 0.1 M monovalent salt, $1/\kappa$ = 0.96 nm at 25 °C.

predicted by the linearized Gouy–Chapman theory falls off exponentially with distance from the membrane, z, according to $\psi = \psi_0 \exp(-\kappa z)$, where ψ_0 is the potential at $z = 0$. The average surface potential is related to the average surface charge density σ by $\psi_0 = \sigma/(\epsilon_r\epsilon_0\kappa)$. Note that the difference between the discrete and smeared-charge potentials calculated from the models decreases rapidly with z, a point discussed in more detail by other authors [e.g., Sauve and Ohki (1979) and Israelachvili (1985)].

The discrete-charge effect illustrated in Figure 1 should manifest itself in the adsorption of ions to charged membranes; the objective of this study was to examine experimentally this effect. The fixed-charge model of Nelson and McQuarrie (1975) predicts that the magnitude of the potentials measured with a given charged probe should be significantly different for positive and negative membranes (see Theory). To test this prediction, we formed positive and negative membranes with surface charge densities and average surface potentials that were identical except for sign. Membranes were formed by mixing the zwitterionic lipid PC with positive or negative lipids. However, there is evidence that sodium binds to negative lipids, such as phosphatidylserine (PS) and phosphatidylglycerol (PG), and that this binding reduces both the charge density and the magnitude of the potential for the PC/PS and PC/PG membranes (Nir et al., 1978; Kurland et al., 1979; Eisenberg et al., 1979; Alvarez et al., 1983; McLaughlin et al., 1983). Thus, we needed to known if the magnitude of the potential of the positive membranes is identical with that of the negative membranes. A number of techniques are available that measure average surface potentials; we made electrophoretic mobility measurements on vesicles to deduce the ζ potential and conductance measurements on planar membranes exposed to a carrier to deduce the change in potential in the middle of the membrane produced by charged lipids.

To test for discreteness-of-charge effects, we determined the adsorption of a monovalent anion, TNS, and a divalent cation, Mn, to positive and negative membranes by making fluorescence and NMR measurements. We have discussed the advantages and disadvantages of these probes in Cafiso et al. (1986). To some extent, we have already tested for discreteness-of-charge effects by studying the adsorption of these anionic and cationic probes to negatively charged membranes (McDaniel et al., 1984, 1986). Each probe molecule and each measurement technique, however, has its own artifacts that complicate the interpretation of results. The advantage of using positive and negative membranes is that the same probe molecule can be used to estimate the discreteness-of-charge effect. In the accompanying paper, Hartsel and Cafiso (1986) describe results obtained with two charged spin-label probes. The work reported in these two papers was planned together, and it represents, to the best of our knowledge, the first test of the discreteness-of-charge effect with positive and negative membranes.

Theory

We calculated theoretically the potential sensed by monovalent and divalent probe molecules when they adsorb to a membrane that has charges fixed in a square lattice. We assumed that the adsorption of the probe molecules, which are present at low concentrations at the surface of the membrane, does not significantly change either the surface potential or the number of binding sites. Therefore, the surface density of adsorbed probe (i.e., [TNS] or [Mn], expressed as number of probes adsorbed per unit surface area of membrane, which is located in the xy plane) should be proportional to the average aqueous concentration (i.e., $\langle$[TNS]$\rangle$ or $\langle$[Mn]$\rangle$) at a small distance, z, from the surface. This interfacial concentration should in turn be related to the probe concentration in the bulk aqueous phase (i.e., $[TNS]_\infty$ or $[Mn]_\infty$) by the average of the Boltzmann factor over the xy plane:

$$\{TNS\} = K_{TNS}\langle[TNS]\rangle = K_{TNS}[TNS]_\infty\langle\exp[F\psi(x,y)/(RT)]\rangle \quad (2)$$

$$\{Mn\} = K_{Mn}\langle[Mn]\rangle = K_{Mn}[Mn]_\infty\langle\exp[-2F\psi(x,y)/(RT)]\rangle \quad (3)$$

$\psi(x,y)$ is the potential at the x,y point a distance z from the membrane surface; K_{TNS} and K_{Mn} are adsorption coefficients;[3] T is absolute temperature, R is the gas constant, and F is Faraday's constant; $\langle\ \rangle$ denotes an average over the xy plane. For neutral PC (phosphatidylcholine) membranes, $\psi(x,y)$ = 0 for $z > 0$, and the average Boltzmann factors in eq 2–3 are equal to unity. If we assume that K_{TNS} and K_{Mn} are the same for charged and neutral membranes, we can describe the adsorption of the probes to PC membranes by

$$\{TNS\}^{PC} = K_{TNS}[TNS]_\infty \quad (4)$$

$$\{Mn\}^{PC} = K_{Mn}[Mn]_\infty \quad (5)$$

We define the effective surface potentials sensed by the idealized probes as ψ_{TNS} and ψ_{Mn}:

$$\psi_{TNS} = (RT/F)\ \ln\ (\langle\exp[F\psi(x,y)/(RT)]\rangle) \quad (6)$$

$$\psi_{Mn} = -[RT/(2F)]\ \ln\ (\langle\exp[-2F\psi(x,y)/(RT)]\rangle) \quad (7)$$

We calculated the theoretically predicted values of ψ_{TNS} and ψ_{Mn} by using a fixed-charge model. We first calculated the potential at all x,y points a given distance from the surface,

[2] This is also the potential predicted by averaging the potentials calculated from the Nelson and McQuarrie (1975) fixed-charge model over a plane parallel to and 0.2 nm away from the membrane surface.

[3] The hydrophobic adsorption of TNS should be described by a Volmer isotherm. The specific adsorption of Mn to the phosphate group of PC should be described by a Langmuir isotherm. However, when the number of adsorbed ions is low, both reduce to the Henry law isotherm given in eq 2–3 (McLaughlin & Harary, 1976).

Table I: Theoretical Predictions of Electrostatic Potential a Distance z from the Surface Calculated from a Smeared-Charge Model (ψ_{SC}) and a Fixed-Charge Model[a]

monovalent salt concn (M)	lattice spacing (nm)	z (nm)	ψ_{SC} (mV)	ψ_{TNS} (mV)	ψ_{Mn} (mV)
0.1	3	0.2	−20	−16	−76
0.1	3	0.2	20	39	15
0.1	3	0.3	−18	−15	−37
0.1	3	0.3	18	24	14
0.1	2	0.2	−45	−40	−97
0.1	2	0.2	45	66	37
0.1	2	0.3	−41	−37	−57
0.1	2	0.3	41	47	36
0.01	3	0.2	−73	−68	−136
0.01	3	0.2	73	96	67
0.01	3	0.3	−71	−67	−94
0.01	3	0.3	71	79	66
0.01	2	0.2	−164	−158	−220
0.01	2	0.2	164	188	155
0.01	2	0.3	−159	−155	−178
0.01	2	0.3	159	166	153

[a] ψ_{TNS} is the potential sensed by a monovalent anion. ψ_{Mn} is the potential sensed by a divalent cation.

z (e.g., z = 0.2 nm) from eq 32 of Nelson and McQuarrie (1975).[4] We then calculated the Boltzmann factor at each x,y point to deduce the concentration of the probes at the distance z. Some representative concentration profiles are illustrated in Nelson and McQuarrie (1975). We then integrated the Boltzmann factor over the xy surface and used eq 6–7 to calculate the theoretically predicted values of ψ_{TNS} and ψ_{Mn}. Table I illustrates these predicted values. If we assume the charge is smeared uniformly over the surface and use the linear Poisson–Boltzmann equation (linear Gouy–Chapman theory), we can calculate the smeared-charge potential ψ_{SC}. The probes underestimate slightly the magnitude of the smeared-charge potential when they are co-ions, that is, when they have the same sign as the surface charge. For example, the first two rows of Table I indicate that TNS senses a potential ψ_{TNS} = −16 mV when the smeared-charge value is −20 mV and Mn senses a potential ψ_{Mn} = 15 mV when the smeared-charge value is 20 mV. The probes significantly overestimate the magnitude of the smeared-charge potential when they are counterions, that is, when they have the opposite sign as the surface charge. For example, row 2 of Table I indicates that TNS senses a potential of 39 mV when the smeared-charge potential is 20 mV. Furthermore, the overestimates are larger for divalent than for monovalent counterions. For example, row 1 indicates that Mn senses a potential ψ_{Mn} = −76 mV when the smeared-charge value is only −20 mV. Other aspects of the discrete-charge model are apparent from Table I. Note that the deviation of ψ_{TNS} and ψ_{Mn} from ψ_{SC} decreases rapidly with distance from the surface (i.e., it is less at 0.3 nm than at 0.2 nm). Finally, note that the deviation is proportionally less when the separation between the charges is small (i.e., less for 2-nm than for 3-nm lattice spacing) and the Debye length is large (i.e., less for 0.01 M than for 0.1 M salt).

We compared our experimental results with the theoretical predictions in Table I. It is clear from eq 2–5 that the surface-averaged Boltzmann factor used in eq 6–7 to calculate ψ_{TNS} and ψ_{Mn} should be equal to the ratio of the number of probes adsorbed to charged and neutral membranes. We determined this ratio experimentally for TNS and Mn (see Materials and Methods) under conditions where the number of adsorbed probes was proportional to the probe concentration in the bulk aqueous phase. This justifies experimentally our assumption that the probes do not significantly change either the surface potential or the number of adsorption sites.

[4] We did not calculate potential or ion concentrations at the membrane surface (z = 0) using the discrete-charge theory because they approach infinity as r approaches zero (see eq 1). We chose distances of 0.2–0.3 nm, the size of atomic radii.

Materials and Methods

Egg or diphytanoylphosphatidylcholine (PC), dimyristoylphosphatidylcholine (DMPC), bovine brain phosphatidylserine (PS), egg phosphatidylglycerol (PG), and dimyristoylphosphatidylglycerol (DMPG) were obtained from Avanti Biochemicals (Birmingham, AL). Hexadecyltrimethylammonium chloride (HTAC) and didodecyldimethylammonium bromide (DDDA) were purchased from Eastman Kodak (Rochester, NY). DDDA was purified by the procedure of Angel et al. (1983). 4-Morpholinepropanesulfonic acid (MOPS) was obtained from P-L Biochemicals (Milwaukee, WI). 2-(*p*-Toluidinyl)naphthalene-6-sulfonate (TNS) and gramicidin D were purchased from Sigma (St. Louis, MO). 2-(*N*-Hexadecylamino)naphthalene-6-sulfonate (HNS) and 4-amino-2,2,6,6-tetramethylpiperidine-1-oxyl (tempamine) were obtained from Molecular Probes (Eugene, OR). Thallium nitrate I ($TlNO_3$) was purchased from Alfa Products (Danvers, MA). Aqueous solutions, prepared with 18 MΩ-cm water (Super-Q, Millipore Corp., Bedford, MA), were buffered to pH 7.3–7.5 with 0.1–5 mM MOPS. We used the following molecular weights in our calculations: PS, 832; egg PG, 775; egg PC, 787; diphytanoyl-PC, 846; DMPC, 678; DMPG, 666; DDDA, 463.

Electrophoretic Mobility Measurements. Multilamellar vesicles for the microelectrophoresis experiments were prepared according to Bangham et al. (1974). Bovine PS, egg PG, DDDA or mixtures of these charged lipids with egg PC in chloroform were vacuum-dried in glass round-bottom flasks. The mobilities of the vesicles were measured in a Rank Brothers Mark I instrument (Bottisham, Cambridge, U.K.) as described previously (McLaughlin et al., 1981). All mobilities are the average of at least two sets of measurements on 10 vesicles. The presence of 10^{-5} M EDTA in the solution did not significantly affect the results. We calculated the ζ potential from the electrophoretic mobility u by using the Helmholtz–Smoluchowski equation (Aveyard & Haydon, 1973; Hunter, 1981):

$$\zeta = u\eta/(\epsilon_r\epsilon_0) \quad (8)$$

where ϵ_r is the dielectric constant of the aqueous solution, ϵ_0 is the permittivity of free space, and η is the viscosity of the aqueous solution. By definition, the ζ potential is the average electrostatic potential at the hydrodynamic plane of shear (Verwey & Overbeek, 1948). We describe the results with the Gouy–Chapman–Stern theory, assuming that the distance from the plane of shear to the charge plane is 0.2 nm (Eisenberg et al., 1979; Rooney et al., 1983; Alvarez et al., 1983). We also assume that the intrinsic association constant of Na with PS and PG is 1.0 M^{-1} (Nir et al., 1978; Kurland et al., 1979; Eisenberg et al., 1979; Alvarez et al., 1983; McLaughlin et al., 1983; McDaniel et al., 1984; Macdonald & Seelig, 1986) and that the intrinsic association constant of Cl with DDDA is 1.0 M^{-1}.

The ζ potentials of PC vesicles in 0.001, 0.01, and 0.1 M NaCl solutions do not differ significantly from zero (Hanai et al., 1965; Bangham, 1968; Eisenberg et al., 1979; McDaniel et al., 1984). In contrast, PC vesicles have a ζ potential of about −3 mV in 0.1 M solutions of $NaNO_3$ or NaBr. The

simplest interpretation is that NO_3 and Br bind more strongly to the choline head group of PC than does Cl. Tatulian (1983) also reported stronger binding of NO_3 and Br than Cl to a PC surface. The ζ potentials of DDDA and egg PC/DDDA vesicles are significantly less positive in 0.1 M $NaNO_3$ or 0.1 M NaBr than in 0.1 M NaCl (unpublished data). For example, the ζ potential of PC/DDDA (5:2 mol/mol) vesicles is 40 mV in 0.1 M NaCl but only 26 mV in either 0.1 M $NaNO_3$ or 0.1 M NaBr. The simplest interpretation is that NO_3 and Br bind more strongly than Cl to the quaternary nitrogen of DDDA, an interpretation consistent with the results of Marra (1986). We report measurements only in NaCl solutions because the positive surface potentials of PC/DDDA membranes are equal in magnitude to the negative potentials of both PC/PS and PC/PG membranes.

Conductance Measurements. Planar lipid bilayers were formed by using a 1% solution of lipid in *n*-decane (McLaughlin et al., 1970, 1971; Cafiso et al., 1986). These optically black films were formed across a 1.6 mm diameter hole in the partition separating two compartments (20 mL each) in a Teflon chamber. The solutions contained 0.1 M KCl or 0.09 M NaCl plus 0.01 M KCl and were buffered to pH 7.3 at 23 °C with 5 mM MOPS. The membrane conductance was measured at low applied potential (25 mV) after addition of $(0.1–1.0) \times 10^{-6}$ M nonactin or FCCP. This conductance is proportional to the equilibrium concentration of nonactin–K or FCCP within the membrane (McLaughlin et al., 1970, 1971, 1977), which depends exponentially on the electrostatic potential within the membrane according to the Boltzmann relation. Thus, the change in electrostatic potential within the membrane upon addition of charged lipid is

$$\Delta\psi = \pm(RT/F) \ln (G/G_0) \quad (9)$$

where G is the conductance of a planar bilayer formed from a mixture of PC and charged lipid and G_0 is the conductance of a PC bilayer. The (−) sign denotes the conductance induced by the positively charged nonactin–K complex, and the (+) sign denotes the conductance induced by the anionic form of the weak acid FCCP. The magnitudes of the conductance changes were approximately equal for the oppositely charged probes. This observation implies that the changes in conductance are due to a change in electrostatic potential within the membrane, which is the sum of the diffuse double layer and dipole potentials. Changes in other parameters, such as the fluidity or dielectric constant of the membrane, would change the nonactin and FCCP conductance in the same direction.

Fluorescence Measurements. We described previously how TNS can be used to estimate the electrostatic potential at the hydrocarbon–water interface of phospholipid bilayers (Eisenberg et al., 1979; McDaniel et al., 1984; Cafiso et al., 1986). This anionic fluorescent probe was added to aqueous solutions containing sonicated vesicles (Barenholz et al., 1977) and either 0.01 or 0.1 M NaCl buffered to pH 7.4 with 0.5 or 5 mM MOPS at 22 °C. The net fluorescence intensity is proportional to the number of TNS molecules adsorbed to the membrane. The ratio of probe molecules adsorbed to a charged surface to those adsorbed to a neutral surface (e.g., PC) should be equal to the surface-averaged Boltzmann factor (see eq 2–5). Thus, the surface potential sensed by TNS, $\Delta\psi_0$, is

$$\Delta\psi_0 = (RT/F) \ln (f/f_0) \quad (10)$$

where f and f_0 are the net fluorescence intensities of TNS adsorbed to membranes formed from PC/charged lipid mixtures and PC, respectively. We assume that the quantum yield of TNS adsorbed to PC, PC/PS, PC/PG, and PC/DDDA vesicles is the same for two reasons. First, fluorescence lifetime measurements demonstrate that the quantum yields of TNS adsorbed to PC, PS, and PG vesicles differ by less than 10% (Eisenberg et al., 1979). Second, corrected emission spectra of TNS adsorbed to PC, PC/PS, PC/PG, and PC/DDDA vesicles are nearly identical (data not shown).

The permeability of PC, PC/PS, and PC/PG membranes to TNS is very low: addition of TNS to a solution of sonicated vesicles produces an essentially instantaneous rise in fluorescence, due to adsorption of TNS to the outer monolayer, but the fluorescence does not increase further for many hours. In contrast, the permeability of PC/DDDA bilayers to TNS is appreciable: TNS accumulates in the vesicles with a $t_{1/2}$ ranging from ~35 min for PC/DDDA (20:1) to ~12 min for PC/DDDA (10:1). We estimated the electrostatic surface potential of the outer monolayer of these positively charged vesicles by measuring fluorescence intensities about 1 min after TNS addition. We restricted our surface potential measurements to membranes formed from mixtures containing less than 10 mol % DDDA, where the net fluorescence was proportional to both the concentration of lipid (≤0.01 mg/mL for PC/DDDA, ≤0.1 mg/mL for PC, PC/PS, and PC/PG mixtures, ≤0.25 mg/mL for PS and PG in 0.1 M NaCl and ≤2 mg/mL in 0.01 M NaCl) and the concentration of TNS (≤0.5 μM) in the bulk aqueous phase, which indicates that TNS does not significantly change the surface potential under our conditions.

We were interested in estimating the surface potential of membranes in the gel state. TNS is not a suitable probe because it adsorbs much less to frozen than to fluid membranes (unpublished observations). Thus, we measured the effect of water-soluble, positively charged quenchers on the fluorescence of a probe bound to the membrane–solution interface. The Stern–Volmer equation predicts

$$F_0/F - 1 = K_{SV}[Q] \quad (11)$$

where F_0 and F are the fluorescence intensities in the absence and presence of quencher, [Q] is the aqueous concentration of quencher adjacent to the fluorophore, and K_{SV} is the Stern–Volmer quenching constant. For a fluorophore completely accessible to a collisional quencher, a plot of $(F_0/F - 1)$ vs. $[Q]_\infty$ yields a straight line, where $[Q]_\infty$ refers to the concentration of the quencher in the bulk aqueous phase. The slope of this line for a neutral PC membrane is equal to K_{SV}. The slope for a charged membrane is equal to $K_{SV} \times \exp[F\Delta\psi_f/(RT)]$ when the quencher is a monovalent cation. $\Delta\psi_f$ is the electrostatic potential sensed by the quenchers adjacent to the fluorophore. If we assume K_{SV} is the same for both PC and charged membranes, we obtain $\Delta\psi_f$.

We used this approach to measure $\Delta\psi_f$ for DMPC/DMPG (10:1 mol/mol) and DMPG membranes relative to DMPC membranes at 30 (liquid-crystalline phase) and at 12 °C (gel phase). DMPC, DMPG, and their mixtures exhibit a sharp phase transition at 23 °C and do not phase separate (Findlay & Barton, 1978; van Dijck et al., 1978). We added a low concentration (1 mol %) of the fluorescent probe HNS to these membranes and studied the ability of thallous ion (Tl) and the protonated form of tempamine to quench the fluorescence. The available evidence suggests that the chromophore of HNS (our unpublished experiments), and the octadecyl version of this probe (Waggoner & Stryer, 1970), is at the membrane–solution interface. Tl and the nitroxide radical in tempamine are powerful quenchers of fluorescence (Moore & Raftery, 1980; Luisetti et al., 1979). We did experiments on sonicated vesicles in 0.1 M $NaNO_3$–5 mM MOPS, pH 7.4. Gramicidin D (0.5 mol %) in the vesicles allowed Tl to diffuse across the

membranes. Thallium and tempamine were added from stock aqueous solutions of $TlNO_3$ or tempamine acetate (pH 7) to a maximum concentration of 20 mM. Corrected fluorescence intensities of HNS were measured (Spex Fluorocomp, Edison, NJ) at 355 nm excitation and 415 nm emission wavelengths.

NMR Measurements. The effect of manganese and other paramagnetic divalent transition metal cations on the line width of the ^{31}P NMR signal from the phosphodiester groups of phospholipid vesicles was described previously (McLaughlin, 1982; Cafiso et al., 1986). Sonicated vesicles were formed by mixing solutions of PC and either PS, PG, or DDDA in chloroform, evaporating the solvent, adding a buffered NaCl solution, sonicating, centrifuging, and equilibrating the outside of the vesicles with a buffered NaCl solution containing known amounts of manganese (McLaughlin et al., 1981) The 0.01 and 0.1 M NaCl solutions were buffered to pH 7.4 at 25 °C with 0.5 and 5 mM MOPS, respectively. We assumed that the ratio of PC to charged lipid in the outer monolayer is the same as the overall ratio of PC to charged lipid. We measured the line width of the broadened ^{31}P resonance from the outside monolayer of the vesicles with a radio-frequency pulse that nulled the ^{31}P NMR signal from phospholipids in the inner monolayer (Lau et al., 1981). We plotted the line width as a function of external manganese concentration. The external manganese concentration varied from 0 to 100 μM for the negative vesicles, from 0 to 300 μM for the zwitterionic vesicles, and from 0 to 900 μM for the positive vesicles. When this relation is linear, as observed, the slope is proportional to the manganese concentration at the phosphodiester group of PC, which is related to the electrostatic potential at this group via the Boltzmann relation. The difference between this potential in a PC and a charged membrane, $\Delta\psi_P$, can be calculated from

$$(1/T_{2P})/(1/T_{2P}^0) = \exp[-2F\Delta\psi_P/(RT)] \qquad (12)$$

where $1/T_{2P}$ and $1/T_{2P}^0$ represent the effects of a known free concentration of manganese on the transverse relaxation rates of the ^{31}P NMR signal from PC/charged lipid vesicles and PC vesicles, respectively. The linearity of the plots of $1/T_{2P}$ and $1/T_{2P}^0$ as a function of the free manganese concentration confirms that the adsorption of manganese does not significantly affect the surface potential under these conditions. $1/T_{2P}$ and $1/T_{2P}^0$ were calculated from the effects of manganese on the observed line widths, $\Delta\nu_P$ and $\Delta\nu_P^0$, with the relations $1/T_{2P} = \pi\Delta\nu_P$ and $1/T_{2P}^0 = \pi\Delta\nu_P^0$. The potential at a specific site at the membrane surface, in this case the phosphodiester group, is terms the "micropotential" to distinguish it from the average value of the potential at the surface of the membrane.

We also used this technique to measure the surface potential of sonicated bilayer vesicles formed from a 10:1 (mol/mol) mixture of DMPC and DMPG in 0.1 M NaCl–5 mM MOPS, pH 7.4. Sonicated vesicles formed from DMPC were used as the control for the calculation of the potential. We did experiments at 35 and 15 °C (i.e., above and below the gel to liquid-crystalline phase transition temperature of 23 °C).

Results

Electrophoretic Mobility Measurements. Figure 2 illustrates the dependence of the ζ potential on lipid composition. The ζ potential is the electrostatic potential at the hydrodynamic slip plane. It is appropriate to calculate ζ from the measured value of the electrophoretic mobility with eq 8 because "relaxation" effects are negligible for these large multilamellar vesicles, the charges are at the surface, and the surface is smooth (Wiersema et al., 1966; O'Brien & White, 1978). The curves illustrate the predictions of the Gouy–Chapman–Stern theory. Note that the theory describes adequately the ζ potentials of both the negative [see also McLaughlin et al. (1981, 1983) and McDaniel et al. (1984)] and the positive vesicles. Although the agreement between the experimental results and the predictions of a simple theory is gratifying, the important feature of the results illustrated in Figure 2 for this study is simply that the ζ potential of a positive membrane is equal in magnitude but opposite in sign to the ζ potential of a negative membrane. Since ζ is the average potential at the slip plane, which is only about 0.2 nm from the surface, these results provide good evidence that the magnitude of the surface potential is also identical for the positive and negative membranes we studied. Thus, DDDA is a suitable positive lipid for our "probe" experiments.

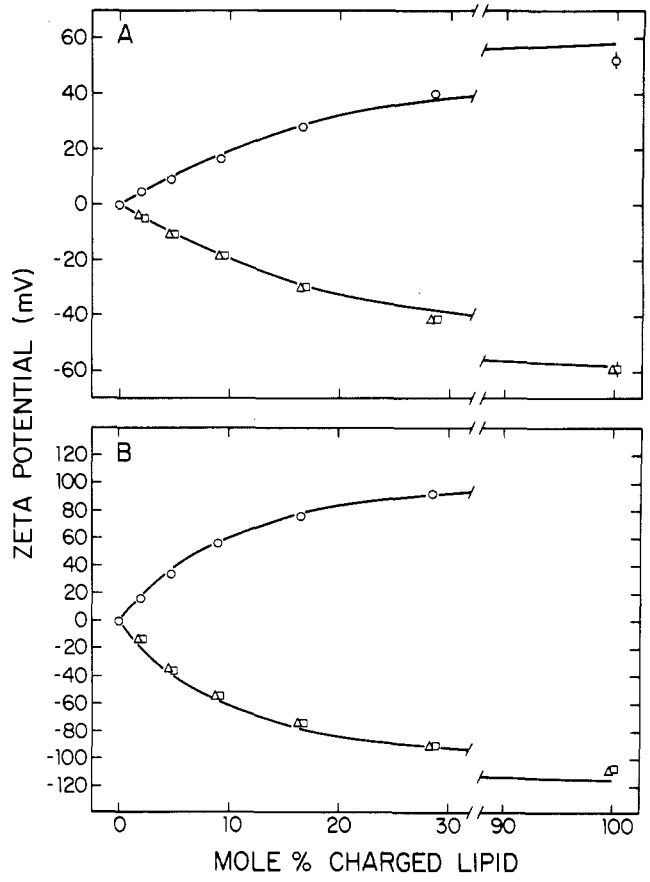

FIGURE 2: ζ potential of multilamellar vesicles formed from mixtures of the zwitterionic lipid PC and the charged lipids PS (squares), PG (triangles), or DDDA (circles). The curves illustrate the predictions of the Gouy–Chapman–Stern theory if the intrinsic association constant of Na with the negative lipids and Cl with the positive lipid is 1 M^{-1} and the plane of shear is 0.2 nm from the membrane surface. The error bars illustrate the standard deviations of measurements on at least 20 vesicles when the deviation is larger than the size of the symbol. The aqueous solutions contained (A) 0.1 and (B) 0.01 M NaCl buffered to pH 7.5 at 25 °C with 1 and 0.1 mM MOPS, respectively.

Conductance Measurements. We made conductance measurements on decane-containing PC, PC/PS, and PC/DDDA planar bilayers to estimate the effect of negative and positive lipids on the electrostatic potential sensed by ions within the membrane. We measured the steady-state conductance due to either the positively charged nonactin–K complex or the negatively charged FCCP anion. This conductance is proportional to the exponent of the potential in the center of the membrane. As we increased the mole fraction of DDDA in the bilayer, the conductance induced by nonactin decreased and the conductance induced by FCCP increased;

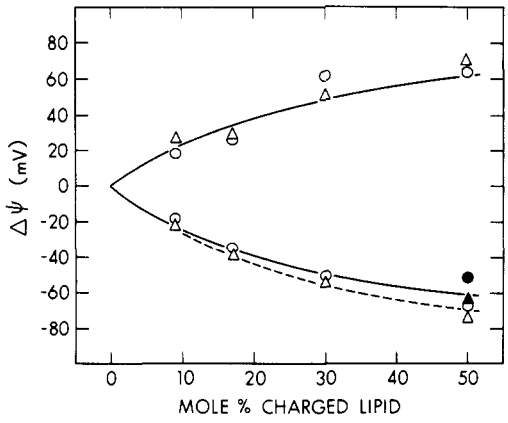

FIGURE 3: Difference between electrostatic potentials within charged planar bilayer membranes and PC membranes. The charged membranes were formed from mixtures of diphytanoyl-PC and either PS (lower half) or DDDA (upper half). The potentials were calculated from steady-state conductance data with eq 9. We made measurements with a negatively charged FCCP probe (triangles) and a positively charged nonactin–K probe (circles). The open symbols represent experiments done in 0.1 M KCl and the filled symbols in 0.09 M NaCl plus 0.01 M KCl. The curves illustrate the predictions of the Gouy–Chapman–Stern theory if the intrinsic association constants are 1 M^{-1} for Cl–DDDA, 1 M^{-1} for Na–PS (solid curve), and 0.5 M^{-1} for K–PS (dashed curve). The symbols represent the average of at least two measurements in solutions buffered to pH 7.3 at 23 °C with 5 mM MOPS.

Table II: Measurements of $\Delta\psi_f$ for Gel and Liquid-Crystalline States of Lipid Bilayer Membranes

		$\Delta\psi_f$ (mV)	
T (°C)	quencher	DMPC/DMPG (10:1)	DMPG
30	Tl^+	−15	−96
12	Tl^+	−16	−98
30	tempamine	−7	−71
12	tempamine	−7	−61

when we increased the mole fraction of PS, the nonactin conductance increased and the FCCP conductance decreased.

Figure 3 illustrates $\Delta\psi$ for PC/PS ($\Delta\psi < 0$) and PC/DDDA ($\Delta\psi > 0$) membranes calculated from conductance measurements with eq 9. The change in electrostatic potential within a PC/DDDA membrane is equal in magnitude but opposite in sign to the change in potential within a PC/PS membrane.

Fluorescence Measurements. Figure 4 illustrates the electrostatic surface potential of sonicated vesicles. The symbols illustrate potentials calculated from fluorescence data (not shown) with eq 10, and the curves illustrate the predictions of Gouy–Chapman–Stern theory for planar surfaces.[5] The most important feature of Figure 4 is the symmetry in potentials reported by TNS for the positively and negatively charged membranes. In 0.01 M NaCl they are symmetic. In 0.1 M NaCl the potentials sensed by TNS for PC/DDDA vesicles are slightly higher than the magnitude of the potentials sensed for PC/PG and PC/PS vesicles.

We obtained measurements of $\Delta\psi_f$ from the quenching of HNS fluorescence by either Tl or tempamine for DMPC/DMPG (10:1) and DMPG membranes. The results for both liquid-crystalline-state and gel-state membranes are shown in Table II.

[5] The Gouy–Chapman equation, which assumes the charges are in a plane, overestimates the magnitude of the potential produced by the charges on the surface of a sphere. The overestimate depends on the ratio of vesicle radius to the Debye length (Ohshima, 1982). For example, for PC/PS (10:1) vesicles of limiting radius, 12.5 nm, the overestimates are only 7% in 0.1 M NaCl and 11% in 0.01 M NaCl.

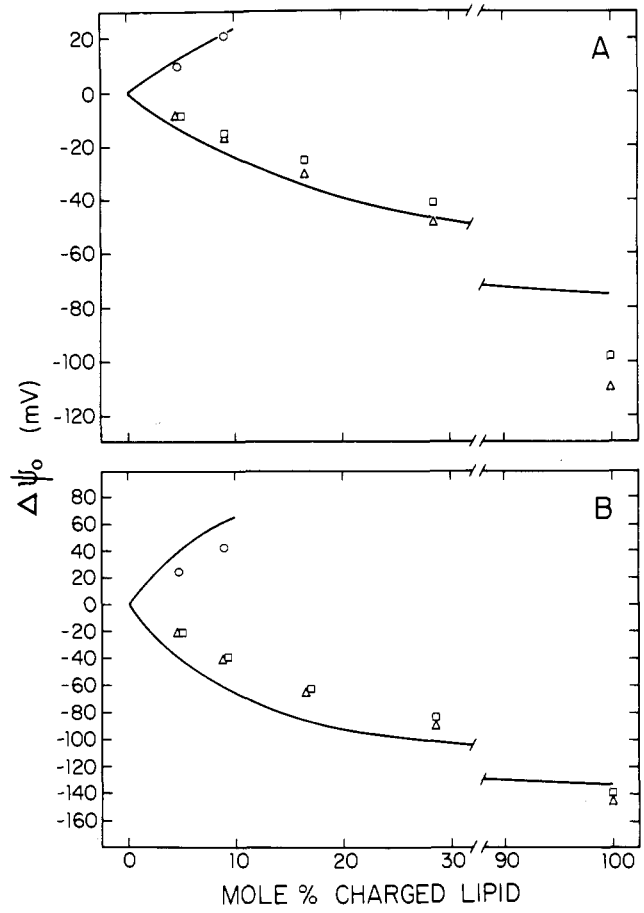

FIGURE 4: Difference between electrostatic surface potentials of charged sonicated unilamellar vesicles and PC vesicles. The charged vesicles were formed from mixtures of PC and either PS (squares), PG (triangles), or DDDA (circles). the values of $\Delta\psi_0$ were determined from fluorescence measurements with the anionic probe TNS by using eq 10. The curves illustrate the predictions of Gouy–Chapman–Stern theory if we assume the intrinsic association constant is 1 M^{-1} for Cl–DDDA, Na–PS, and Na–PG. The symbols represent the average of two or more measurements. The aqueous solutions contained (A) 0.1 and (B) 0.01 M NaCl buffered to pH 7.4 at 22 °C with 5 and 0.5 mM MOPS, respectively.

NMR Measurements. Figure 5 summarizes NMR results obtained with sonicated vesicles. We measured similar potentials for PC/PS and PC/PG membranes, in agreement with the ζ potential and fluorescence results. All measured $\Delta\psi_P$ values are less than the values predicted from Gouy–Chapman–Stern theory, a result we do not understand. The magnitudes of the $\Delta\psi_P$ values for PC/DDDA membranes are approximately equal to the corresponding values for the negatively charged membranes.

We also measured potentials for DMPC/DMPG (10:1) membranes above and below their phase transition. $\Delta\psi_P$ was calculated to be −23 mV at 35 °C (liquid-crystalline state) and −27 mV at 15 °C (gel state). Neither fluorescence (Table II) nor NMR measurements reveal any striking changes in the surface potential of membranes going from the liquid-crystalline to the gel state.

DISCUSSION

We saw no evidence of discrete-charge effects when we compared the number of charged probes adsorbed to positive and negative membranes. A simple theory (Nelson & McQuarrie, 1975) predicted that the discrete nature of charges fixed in a regular lattice should markedly affect the adsorption of counterions, particularly divalent counterions, to charged membranes (see lines 1 and 2 of Table I). Our results with

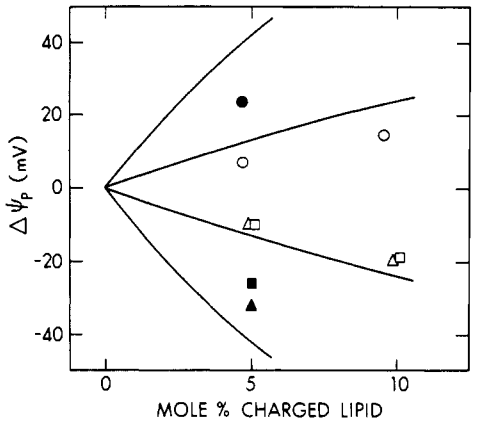

FIGURE 5: Difference between electrostatic potential at the phosphodiester group of PC in charged and neutral sonicated vesicles. The charged vesicles were formed from mixtures of PC and either PS (squares), PG (triangles), or DDDA (circles). the values of $\Delta\psi_P$ were determined from ^{31}P NMR measurements with eq 12. The aqueous solutions contained either 0.01 (filled symbols) or 0.1 M NaCl (open symbols) buffered to pH 7.4 at 25 °C with 0.5 or 5 mM MOPS, respectively. The curves illustrate the predictions of the Gouy–Chapman–Stern theory if the intrinsic association constant is 1 M^{-1} for Cl–DDDA, Na–PS, and Na–PG.

monovalent (Figure 4) and divalent probes (Figure 5), and the results in the accompanying paper (Hartsel & Cafiso, 1986) with a matched pair of positive and negative spin-labeled probes, agree much more closely with the predictions of the Gouy–Chapman–Stern (GCS) theory, in which the charges on a membrane are assumed to be smeared uniformly over the surface.

Previous experimental studies have also failed to detect any evidence for discreteness-of-charge effects with phospholipid bilayers. Consider first the effect of a 10-fold increase in the concentration of counterions on the surface or ζ potential of negatively charged membranes. The GCS theory predicts a maximum change in potential of $2.3RT/(ZF)$, where Z is the valence of the cation. Thus for monovalent, divalent, and tetravalent cations, the potential should change by about 58, 29, and 14 mV at 25 °C. A discrete-charge calculation predicts the change in potential should be larger than $2.3RT/(ZF)$, as discussed, for example, by Barlow and McDonald (1967). An anomalously large change in potential per 10-fold change in salt concentration is referred to as an Esin–Markov effect after the authors who first reported such effects. A variety of experimental approaches provide strong evidence that the changes in potential observed on bilayer membranes and monolayers with monovalent (Davies, 1951; Eisenberg et al., 1979; Lakhdar-Ghazal et al., 1983; Figures 2, 4, and 5 of this paper), divalent (McLaughlin, 1977; Ohki & Sauve, 1978; McLaughlin et al., 1981; Lau et al., 1981), and tetravalent (Chung et al., 1985) cations agree with, or are slightly less than, the values predicted by GCS theory. The GCS theory is successful not only with inorganic ions such as sodium and calcium but with a variety of amphipathic ions that adsorb hydrophobically to membranes. These ions include both negative and positive detergents (Haydon & Myers, 1973; McLaughlin, 1977), local anesthetics (McLaughlin, 1975), fluorescent probes such as TNS (McLaughlin & Harary, 1976) and ANS (Gibrat et al., 1983), and a variety of uncouplers of oxidative phosphorylation (Bakker et al., 1975; Cohen et al., 1977, Dilger et al., 1979; Benz & McLaughlin, 1983; Kasianowicz et al., 1984). No Esin–Markov effects were observed in any of these studies.

Consider next force measurements between surfaces. Direct measurements of the force between charged mica sheets can be described by a smeared-charge theory, even when the sheets are closer to each other than the mean distance between the surface charges and no counterions are present [see p 192 of Israelachvili (1985)]. Similar good agreement with smeared-charge calculations is obsered with direct force measurements on mica sheets coated with a lipid bilayer (Marra & Israelachvili, 1985) and with multilammelar phospholipid systems (Loosley-Millman et al., 1982).

Why does the smeared-charge theory work so well for phospholipid bilayers? Several factors might be important. First, the difference between potentials calculated from smeared-charge and discrete-charge models decays rapidly with either distance from the surface (see Figure 1) or distance on the surface from a fixed charge. All measurements of the surface potential reported here and in the accompanying paper (Hartsel & Cafiso, 1986) must be influenced by the finite size of the lipids, which occupy areas of about 0.6–0.7 nm^2. We made discreteness-of-charge calculations by assuming the probe molecules were excluded from squares of area 0.64 nm^2 centered on the surface charges. For example, when the monovalent salt concentration was 0.1 M, the lattice spacing was 3 nm, and the distance from the surface was 0 nm, the average surface potential calculated from a smeared-charge theory [$\psi_0 = \sigma/(\epsilon_r\epsilon_0\kappa)$] is 25 mV while the average surface potential, $\langle\psi_0(x,y)\rangle$, calculated from a discrete-charge model (Nelson & McQuarrie, 1975), excluding an area of 0.64 nm^2 around the fixed charges, is 16 mV. The potentials sensed by TNS and Mn are predicted to be $\psi^0_{TNS} = -15$ mV and $\psi^0_{Mn} = -22$ mV for negative membranes and $\psi^0_{TNS} = 18$ mV and $\psi^0_{Mn} = 14$ mV for positive membranes. The superscript 0 indicates that these averages were calculated at $z = 0$ (see eq 6–7); the values listed in Table I were calculated at $z = 2$ and 3 nm. These predicted values of ψ^0_{TNS} and ψ^0_{Mn}, which take into account the finite size of the lipids, agree more closely with the predictions of the smeared-charge model (and the experimental results) than do the predictions from the discrete-charge model (Nelson & McQuarrie, 1975) illustrated in Table I (see rows 1 and 2). We suspect this is the main reason we observed such good agreement of our experimental results with the smeared-charge theory. Second, the existing theories do not take into account the lateral mobility of the surface charges, which may effectively smear the charge over the surface. Sophisticated mobile discrete-charge theories are being developed following the outline of Kjellander and Marcelja (1986) (S. Marcelja, personal communication). However, we saw little difference between the surface potential of bilayer membranes in the gel and liquid-crystalline state, which suggests this factor is not of major importance. Third, a variety of other factors exist that may be important; many are discussed in the extensive reviews on this topic [e.g., Levine et al. (1963), Stigter (1964), and Barlow and McDonald (1967)]. In particular, ion–ion correlations, which are not considered in the Poisson–Boltzmann equation, may be important (S. Marcelja, personal communication).

We do not wish to imply that discrete-charge effects will never be important to membrane biologists. These effects become important if the charges are buried within the low dielectric interior of the bilayer. A low density of such charges produces a large boundary potential [e.g., McLaughlin (1977)], and significant Esin–Markov effects have been observed when hydrophobic ions such as tetraphenyl borate or dipicrylamine adsorb to membranes (Andersen et al., 1978; Wang & Bruner, 1978). These effects can be described adequately by the mobile discrete-charge theory of Tsien and Hladky (1982). Discrete-charge effects should also become

important when the valence on the adsorbing ion is large, even if it remains at the surface. In fact, such effects were observed when the hexavalent polypeptide melittin adsorbs to planar lipid bilayers (Schoch & Sargent, 1980). Finally, a number of authors have pointed out that discrete-charge effects should be important with respect to proteins (Warshel, 1984; Matthew, 1985; Honig & Hubbell, 1986), particularly proteins that form channels in membranes (Cole, 1969; Hille, 1972; Neumcke, 1976; Attwell & Eisner, 1978; Dani, 1986). We agree. However, the experiments reported here strongly suggest that the classical Gouy–Chapman–Stern theory, with its assumption the charges are smeared uniformly over a planar surface, is adequate to describe the electrostatic properties of lipid bilayer membranes and, by inference, the bilayer component of biological membranes.

ACKNOWLEDGMENTS

We thank Gerard Vaio for excellent technical assistance with some of the experiments, Dr. Stjepan Marcelja for valuable discussions about his unpublished theoretical calculations, and Dr. Richard Mathias for helpful comments about the manuscript.

Registry No. DDDA, 3282-73-3; DMPC, 13699-48-4; DMPG, 61361-72-6; diphytanoyl-PC, 64626-70-6.

REFERENCES

Alvarez, O., Brodwick, M., Latorre, R., McLaughlin, A., McLaughlin, S., & Szabo, G. (1983) *Biophys. J. 44*, 333–342.

Andersen, O. S., Feldberg, S., Nakadomari, H., Levy, S., & McLaughlin, S. (1978) *Biophys. J. 21*, 35–70.

Angel, L. R., Evans, D. F., & Ninham, B. W. (1983) *J. Phys. Chem. 87*, 538–540.

Attwell, D., & Eisner, D. (1978) *Biophys. J. 24*, 869–875.

Aveyard, R., & Haydon, D. A. (1973) *Introduction to the Principles of Surface Chemistry*, pp 40–57, Cambridge Press, Cambridge, U.K.

Bakker, E. P., Arents, J. C., Hoebe, J. P. M., & Terada, H. (1975) *Biochim. Biophys. Acta 387*, 491–506.

Bangham, A. D. (1968) *Prog. Biophys. Mol. Biol. 18*, 29–95.

Bangham, A. D., Hill, M. W., & Miller, N. G. A. (1974) *Methods Membr. Biol. 1*, 1–68.

Barenholz, Y., Gibbes, D., Litman, B. J., Goll, J., Thompson, T. E., & Carlson, F. D. (1977) *Biochemistry 16*, 2806–2810.

Barlow, C. A., & MacDonald, J. R. (1967) *Adv. Electrochem. Electrochem. Eng. 6*, 1–199.

Belaya, M. L., & Feigelman, M. V. (1985) *Biol. Membr. 1*, 303–312.

Benz, R., & McLaughlin, S. (1983) *Biophys. J. 41*, 381–398.

Brown, R. H. (1974) *Prog. Biophys. Mol. Biol. 28*, 343–370.

Cafiso, D., McLaughlin, A., McLaughlin, S., & Winiski, A. (1986) *Methods Enzymol.* (in press).

Chung, L., Kaloyanides, G., McDaniel, R., McLaughlin, A., & McLaughlin, S. (1985) *Biochemistry 24*, 442–452.

Cohen, F. S., Eisenberg, M., & McLaughlin, S. (1977) *J. Membr. Biol. 37*, 361–396.

Cole, K. S. (1969) *Biophys. J. 9*, 465–469.

Dani, J. A. (1986) *Biophys. J. 49*, 607–618.

Davies, J. T. (1951) *Proc. R. Soc. London, Ser. A 208*, 224–247.

Dilger, J., & McLaughlin, S. (1979) *J. Membr. Biol. 46*, 359–384.

Duniec, J. T., & Thorne, S. W. (1983) *Bull. Math. Biol. 45*, 69–90.

Eisenberg, M., Gresalfi, T., Riccio, T., & McLaughlin, S. (1979) *Biochemistry 18*, 5213–5223.

Findlay, E. J., & Barton, P. G. (1978) *Biochemistry 17*, 2400–2405.

Gibrat, R., Romieu, C., & Grignon, C. (1983) *Biochim. Biophys. Acta 736*, 196–202.

Grahame, D. C. (1958) *Z. Elektrochem. 62*, 264–274.

Hanai, T., Haydon, D. A., & Taylor, J. (1965) *J. Theor. Biol. 9*, 278–296.

Hartsel, S. C., & Cafiso, D. S. (1986) *Biochemistry* (following paper in this issue).

Haydon, D. A., & Myers, V. B. (1973) *Biochim. Biophys. Acta 307*, 429–443.

Hille, B. (1972) *J. Gen. Physiol. 59*, 637–658.

Honig, B., Hubbell, W. L., & Flewelling, R. F. (1986) *Annu. Rev. Biophys. Biophys. Chem. 15*, 163–193.

Hunter, R. J. (1981) *Zeta Potential in Colloid Science*, Academic, New York.

Israelachvili, J. N. (1985) *Intermolecular and Surface Forces*, pp 191–193, Academic, New York.

Kasianowicz, J., Benz, R., & McLaughlin, S. (1984) *J. Membr. Biol. 82*, 179–190.

Kjellander, R., & Marcelja, S. (1986) *Chem. Phys. Lett. 127*, 402–407.

Kurland, R., Newton, C., Nir, S., & Papahadjopoulos, D. (1979) *Biochim. Biophys. Acta 551*, 137–147.

Lakhdar-Ghazal, F., Tichadou, J.-L., & Tocanne, J.-F. (1983) *Eur. J. Biochem. 134*, 531–537.

Lau, A., McLaughlin, A., & McLaughlin, S. (1981) *Biochim. Biophys. Acta 645*, 279–292.

Levine, S., Mingins, S., & Bell, G. M. (1967) *J. Electroanal. Chem. 13*, 280–329.

Loosley-Millman, M. E., Rand, R. P., & Parsegian, V. A. (1982) *Biophys. J. 40*, 221–232.

Luisetti, J., Mohwald, H., & Galla, H.-J. (1979) *Biochim. Biophys. Acta 552*, 519–530.

Macdonald, P. M., & Seelig, J. (1986) *Biochemistry* (submitted for publication).

Marra, J. (1986) *J. Phys. Chem. 90*, 2145–2150.

Marra, J., & Israelachvili, J. N. (1985) *Biochemistry 24*, 4608–4618.

Matthew, J. B. (1985) *Annu. Rev. Biophys. Biophys. Chem. 14*, 387–417.

McDaniel, R. V., McLaughlin, A., Winiski, A. P., Eisenberg, M., & McLaughlin, S. (1984) *Biochemistry 23*, 4618–4624.

McDaniel, R. V., Sharp, K., Brooks, D., McLaughlin, A. C., Winiski, A. P., Cafiso, D., & McLaughlin, S. (1986) *Biophys. J. 49*, 741–752.

McLaughlin, A. C. (1982) *Biochemistry 21*, 4879–4885.

McLaughlin, A., Eng, W.-K., Vaio, G., Wilson, T., & McLaughlin, S. (1983) *J. Membr. Biol. 76*, 183–193.

McLaughlin, S. (1975) *Prog. Anesthesiol. 1*, 193–221.

McLaughlin, S. (1977) *Curr. Top. Membr. Transp. 9*, 71–144.

McLaughlin, S., & Harary, H. (1976) *Biochemistry 15*, 1941–1948.

McLaughlin, S., Mulrine, N., Gresalfi, T., Vaio, G., & McLaughlin, A. (1981) *J. Gen. Physiol. 77*, 445–473.

McLaughlin, S. G. A., Szabo, G., Eisenman, G., & Ciani, S. M. (1970) *Proc. Natl. Acad. Sci. U.S.A. 67*, 1268–1275.

McLaughlin, S. G. A., Szabo, G., & Eisenman G. (1971) *J. Gen. Physiol. 58*, 667–687.

Moore, H.-P. H., & Raftery, M. A. (1980) *Proc. Natl. Acad. Sci. U.S.A. 77*, 4509–4513.

Nelson, A. P., & McQuarrie, D. A. (1975) *J. Theor. Biol. 55*, 13–27.

Neumcke, B. (1976) *J. Electrochem. Soc. 123*, 1331–1334.

Nir, S., Newton, C., & Papahadjopoulos, D. (1978) *Bioelectrochem. Bioenerg. 5*, 116-133.
O'Brien, R. W., & White, L. R. (1978) *J. Chem. Soc., Faraday Trans. 2 74*, 1607-1626.
Ohki, S., & Sauve, R. (1978) *Biochim. Biophys. Acta 511*, 377-387.
Ohshima, H., Healy, T. W., & White, L. R. (1982) *J. Colloid Interface Sci. 90*, 17-26.
Rooney, E. K., East, J. M., Jones, O. T., McWhirter, J., Simmonds, A. C., & Lee, A. G. (1983) *Biochim. Biophys. Acta 728*, 159-170.
Sauve, R., & Ohki, S. (1979) *J. Theor. Biol. 81*, 157-179.
Schoch, P., & Sargent, D. F. (1980) *Biochim. Biophys. Acta 602*, 234-247.
Stigter, D. (1964) *J. Phys. Chem. 68*, 3603-3611.
Tatulian, S. A. (1983) *Biochim. Biophys. Acta 736*, 189-195.
Tsien, R. Y., & Hladky, S. B. (1982) *Biophys. J. 39*, 49-56.
Van Dijck, P. W M., de Kruijff, B., Verkleij, A. J., van Deenen, L. L. M., & de Gier, J. (1978) *Biochim. Biophys. Acta 512*, 84-96.
Verwey, E. J. W., & Overbeek, J. Th. G. (1948) *Theory of the Stability of Lyophobic Colloids*, Elsevier, Amsterdam.
Waggoner, A. S., & Stryer, L. (1970) *Proc. Natl. Acad. Sci. U.S.A. 67*, 579-589.
Wang, C.-C., & Bruner, L. J. (1978) *Biophys. J. 24*, 749-764.
Warshel, A., & Russell, S. T. (1984) *Q. Rev. Biophys. 17*, 283-422.
White, D. A. (1973) in *Form and Function of Phospholipids* (Ansell, G. B., Hawthorne, J. N., & Dawson, R. M. C., Eds.) pp 441-482, Elsevier, Amsterdam.
Wiersema, P. H., Loeb, A. L., & Overbeek, J. Th. G. (1966) *J. Colloid Interface Sci. 22*, 78-99.

A Test of Discreteness-of-Charge Effects in Phospholipid Vesicles: Measurements Using Paramagnetic Amphiphiles†

Scott C. Hartsel and David S. Cafiso*
Department of Chemistry and Biophysics Program, University of Virginia, Charlottesville, Virginia 22901
Received July 10, 1986

ABSTRACT: A new series of negatively charged, paramagnetic alkylsulfonate probes was synthesized and can be used to measure both the internal and the external surface potentials of model membrane systems. We tested for discreteness-of-charge effects in lipid membranes by comparing the surface potentials, estimated by use of these negatively charged amphiphiles, with that of a series of positively charged alkylammonium nitroxides in charged membranes. From the partitioning of these probes, the membrane surface potential was estimated in phosphatidylcholine membranes containing either phosphatidylserine or didodecyldimethylammonium bromide. The surface potentials, estimated with either positive or negative probes, were identical, within experimental error, in either positive or negative membranes, and they were well accounted for by a simple Gouy-Chapman-Stern theory. This symmetry, with respect to the sign of the charge, indicates that discreteness-of-charge effects are not significant in determining the potential-sensitive phase partitioning of these probes in model membranes. Thus, despite the fact that charge on membranes is discrete, models that assume a uniform density of charge in the plane of the membrane adequately account for the potentials measured by these amphiphilic probes.

Molecular probe techniques provide a powerful methodology for the determination of membrane electrical properties; for example, a number of procedures using fluorescence, EPR,[1] or NMR can be used to estimate the potential at the membrane surface (Castle & Hubbell, 1976; Eisenberg et al., 1979; McDaniel et al., 1984; McLaughlin, 1982; Cafiso & Hubbell, 1981; Cafiso et al., 1986). The surface potential is extremely important in biological systems, affecting processes such as ion conduction, the gating of channels, and the pH or ion concentrations at the membrane-solution interface. This potential is a consequence of fixed-charge density associated with lipid or protein at the membrane-solution interface (McLaughlin, 1977). By use of fluorescent or EPR probes that exhibit a potential-dependent phase partitioning, the surface potential in biological and model membrane vesicles can be estimated. To relate this potential to a charge density at the membrane-solution interface, a simple Gouy-Chapman-Stern model is often employed. This model assumes that charge is uniformly distributed over the surface of the membrane and includes a correction for the absorption of ions to the membrane-solution interface. While this theory clearly ignores the discrete nature of charge on the membrane surface, it nonetheless appears to account for the behavior of certain paramagnetic probes. For example, the phase partitioning of positive alkylammonium nitroxides in negatively charged membranes is well accounted for by this simple theory (Castle & Hubbell, 1976; Gaffney & Mich, 1976; McDaniel et al., 1986).[2] On the other hand, for certain negatively charged

† This work was supported by Grant BNS 8302840 from the National Science Foundation and a grant from the Dreyfus Foundation for New Faculty in Chemistry (to D.S.C.).
* Address correspondence to this author at the Department of Chemistry.

[1] Abbreviations: EPR, electron paramagnetic resonance; NMR, nuclear magnetic resonance; egg PC, egg phosphatidylcholine; PS, phosphatidylserine; HTAC, hexadecyltrimethylammonium chloride; DDDA, didodecyldimethylammonium; TLC, thin-layer chromatography; MOPS, 3-(*N*-morpholino)propanesulfonate.

0006-2960/86/0425-8214$01.50/0